The 2014 World Congress on
Advances in Civil, Environmental, and Materials Research (ACEM14)
Busan, Korea, August 24-28, 2014

Effectiveness and mechanisms of naphthalene adsorption by biochar pyrolyzed from wheat straw

*Yu-Feng Jiang[1)], Xue-Fei Hu[2)] , Uwamungu Yves[3)]

[1), 2), 3)] *Department of Environmental Engineering, Lanzhou Jiaotong University, Lanzhou 730070, China*
[1)] *jiangyf7712@126.com*

ABSTRACT

The objective of this study was to investigate the adsorption of naphthalene by biochar produced from pyrolytic wheat residue at varying temperature. The dynamic and thermodynamic adsorption experiments were conducted to investigate the adsorption characteristics of naphthalene by biochar. The result suggested that the surface feature and the chemical structure of biochar were modified at varying pyrolytic temperature. The kinetic data showed the adsorption of naphthalene onto biochar could be described by a pseudo-second-order kinetic model, and the boundary layer control and intraparticle diffusion are involved in the adsorption simultaneously. Besides, the adsorption thermodynamics fitted well with the Freundlich isothermal model. The saturated adsorption capacity was improved with the increase of systematic temperature, suggesting that adsorption was an endothermic process. Thermodynamic parameters analysis also showed the adsorption was mainly physical adsorption. The biochar produced by pyrolytic wheat residue showed a considerable potential for the naphthalene adsorption.

Keywords: Biochar, Pyrolysis, Adsorption, Thermodynamics, Naphthalene.

1. INTRODUCTION

Biochar as a form of black carbon is a ubiquitous form of carbon comprising of polyaromatic to elemental or graphitic carbon, compared with organic carbon which forms covalent bonds with other elements (Chun et al. 2004; Lehmann and Joseph, 2009; Mohan et al., 2014). Biochar is quite similar to activated carbon with respect to mutual production via pyrolysis, with microporosity and high surface areas (Cao et al., 2011). Additionally, the biochar contains a non-carbonized fraction that may interact with organic pollutants. Specifically, the biochar also contains the carboxyl, hydroxyl, and phenolic surface functional groups that could effectively bind with pollutants (Mohan et al., 2014). Thus, biochar can be effective in sorption of organic pollutants such as dyes, aromatics, polychlorinated biphenyls, pesticides and petroleum hydrocarbons (Ahmad et al. 2012, 2013, 2014; Zhao et al. 2013; Zhang et al. 2013). Previous studies focus on

[1)] Professor
[2)] Graduate Student

adsorption of aqueous organic pollutants which mainly cover dyes, phenolics, pesticides, polynucelar aromatics and antibiotics (Ahmad et al. 2012, 2013, 2014; Mohan et al. 2014; Zhao et al. 2013; Zhang et al. 2013). But the surface properties and adsorptive characteristics may differ widely among biochar produced under varying conditions from different raw materials (Yang and Sheng, 2003; Ahmad et al. 2014; Mohan et al. 2014). Several mechanisms explaining the interactions between biochar and pollutants have been summarized (Ahmad et al. 2014). The major mechanisms controlling the fate of organic pollutants are the partitioning or adsorption because of biochar's high surface area and microporosity, and electrostatic interaction between biochar and organic pollutants (Yang and Sheng, 2003; Uchimiya et al. 2010; Ahmad et al. 2012, 2013, 2014). Polar pollutants were adsorbed via the H-bonding between the pollutants and the O-containing moieties biochar (Sun et al. 2012; Uchimiya et al. 2011).

In Northwest China, because of petroleum industrial activities in the study areas, many petroleum pollutants are generated in the environment, deteriorating ecosystems. Therefore, understanding the adsorption behavior of petroleum pollutants is vital to predict their transport and fate in water. The primary objective of this study is to investigate the adsorption of naphthalene by biochar produced by pyrolyzing wheat residue at varying temperature. The kinetic and equilibrium data for the adsorption experiments were processed to understand the adsorption mechanism of naphthalene by biochar.

2. MATERIALS AND METHODS

2.1 Preparation of biochar samples

Wheat residue was collected from farmland in Gansu province, China. The wheat residue was washed with distilled water four times, air-dried in a greenhouse for 2 days, and then oven-dried overnight at 80 ℃. Some of treated wheat residue was weighed in a crucible, and covered with a fitting lid, then pyrolyzed under the oxygen-limited condition for 4 h at 200, 400, 600 °C, respectively. During the heating process, the treated wheat residue was heated at 100 °C for 1 h, and then increased temperatures to the corresponding temperature. The yield of each bio-product was defined as the ratio of the weight of the product to that of the original wheat residue. Under three pyrolytic temperatures (200, 400, and 600 °C), the yields of biochar from the wheat residue were about 83%, 24%, and 21%, respectively. The biochar samples are hereafter referred to as BC-200, BC-400 and BC-600, respectively, where the suffix X00 (X = 2, 4, 6) to BC represents the pyrolytic temperature when the BC represent biochar. All biochar samples were sieved through 100 meshes.

The surface of char samples were scanned by JSM-5600LV low vacuum scanning electron microscope (SEM, Japan). For each analysis the voltage was set at 20 keV, while the working distance was 9 mm and the dead time for X-ray acquisition between 20% and 25%. Fourier transform infrared (FTIR) spectra were obtained using Bruker Vertex 70 spectrometer (Bruker Optics, Billerica, MA) fitted with a Pike Technologies MIRacle attenuated total reflectance (ATR) accessory (Madison, WI) with a diamond crystal plate. The spectra were obtained at 8 cm^{-1} resolution from 650 to 4500 cm^{-1} with 128 scans. Before FTIR analyses, all samples were adjusted to pH 3.0 and dried overnight at 70 °C.

2.2 Adsorption experiments

Adsorption kinetics and thermodynamics of naphthalene by biochar was determined using a batch equilibrium method. Batch experiments of adsorption kinetics were conducted at 25±0.5℃ in an incubator shaker. A 0.200 g of biochar samples was added to 100-mL plastic screw-capped bottles with 50 mL aqueous solution of naphthalene. The reaction mixture was incubated with stirring (140 rpm). The mixed samples were collected at reaction times of 0, 0.5, 1, 2, 6, 12, 20, 24, 36, 72 h, respectively, and then the solid and liquid were immediately separated at 4000 rpm by a centrifuge. The adsorption isotherm experiments were explained under constant agitation rate (140 rpm), initial pH (7.0±0.5), and three temperatures (25, 35, and 45 °C), and it was conducted with an initial naphthalene concentration ranging from 0 to 48 $mg \cdot L^{-1}$. The solid and liquid phases in all experiments were separated at 4000 rpm by a centrifuge after a given time. Finally the liquid phase was analyzed for naphthalene concentration by an UV spectrophotometer. All experiments were carried out in triplicate.

2.3 Adsorption kinetic model

Kinetic adsorption is one major characteristic affecting the adsorption efficiency. The kinetic data can be used to determine the presence or absence of intraparticle diffusion and whether it is the rate-controlling step. Three kinetic adsorption models including the pseudo-first-order, pseudo-second-order and intraparticle diffusion models were applied with the experimental data to predict the adsorption kinetics and mechanism.

The pseudo-first-order rate equation is expressed as follows (Ho and McKay 1998a; 1998b):

$$\frac{1}{q_t} = \frac{1}{q_1} + \left(\frac{k_1}{q_1 \times t}\right) \tag{1}$$

where q_1 and q_t are the amounts of naphthalene adsorbed at equilibrium and at time t (mg g^{-1}) and k_1 is the adsorption constant (min^{-1}).

The pseudo-second-order kinetic model (Ho and McKay 1998c) is expressed as:

$$\frac{t}{q_t} = \frac{t}{q_2} + \left(\frac{1}{(q_2)^2 \times k_2}\right) \tag{2}$$

where q_2 is the maximum adsorption capacity (mg g^{-1}); q_t is the amount of naphthalene adsorbed at equilibrium at time t (mg g^{-1}); k_2 is the equilibrium rate constant (g mg^{-1} min^{-1}).

The intraparticle diffusion equation (Weber Jr. and Morriss 1963) is written as follows:

$$q_t = k_p \times t^{1/2} + C \tag{3}$$

where C is the intercept and k_p is the rate constant (mg g^{-1} $min^{-1/2}$).

2.4 Adsorption thermodynamic model

The equilibrium adsorption isotherms are one major type of data for understanding the adsorption mechanism (Özcan et al. 2005). Three isotherm equations (Freundlich's, Langmuir's, and Dubinin- Radushkevich, D-R) were chosen in this study.

Langmuir adsorption model is based on the assumption that the maximum adsorption corresponds to a saturated monolayer of molecules on the adsorbent surface, with no lateral interaction between adsorbed molecules (Langmuir 1918). The Langmuir equation for homogenous surface is expressed as follows:

$$\frac{1}{c_s} = \frac{1}{K_L \times q_m \times c_e} + \frac{1}{q_m} \tag{4}$$

where c_s is the adsorption quantity of naphthalene by biochar (mg·g^{-1}); q_m is the saturated adsorption quantity of naphthalene by biochar (mg·g^{-1}); c_e is the equilibrium concentration of naphthalene in aqueous solution, mg·L^{-1}; K_L is Langmuir thermodynamic equilibrium constant.

The Freundlich isotherm model is an empirical equation used to describe heterogeneous surfaces (Freundlich 1906):

$$\lg q_s = \lg K_F + \frac{1}{n} \times \lg c_e \tag{5}$$

where c_s is the adsorption quantity of naphthalene by biochar (mg·g^{-1}); c_e is the equilibrium concentration of naphthalene in aqueous solution (mg·L^{-1}); K_F and n are constants related to biochar properties.

The equilibrium data were also processed by the D-R model to determine the nature of adsorption as physical or chemical. The linear form of the D-R model is expressed as follows (Dubinin et al. 1947):

$$\ln c_s = \ln q_m - \beta \times \varepsilon^2 \tag{6}$$

where c_s is the amount of naphthalene adsorbed by biochar (mol g^{-1}), q_m is the maximum adsorption capacity (mol g^{-1}), β is the activity coefficient related to mean free energy of adsorption (mol^2 J^{-2}) and $\varepsilon = RT\ln(1 + 1/C_e)$ is the Polanyi potential. The mean free energy (E, kJ mol^{-1}) was calculated using β (Helfferich 1979):

$$E = \frac{1}{\sqrt{(-2\beta)}} \tag{7}$$

E provides information about the adsorption mechanism: physical (< 8 kJ mol^{-1}) or chemical (8 - 16 kJ mol^{-1}) (Kiran et al. 2006).

Langmuir isotherm, a method calculating the dimensionless equilibrium constant or separation factor, R_L, is used to reveal the essential characteristics of Langmuir isotherm and can be calculated as follows (McKay et al. 1982):

$$R_L = \frac{1}{(1 + K_L \times c_0)} \tag{8}$$

2.5 Analysis of thermodynamic parameters

Thermodynamic parameters can improve our understanding on the inherent energetic changes involved in the adsorption (Fasfous et al. 2010). To assess the thermodynamic parameters, we measured the adsorption isotherms of biochar at 25, 35, and 45 °C and calculated the changes of thermodynamic parameters including free energy of sorption (ΔG^{θ}), standard enthalpy (ΔH^{θ}) and standard entropy changes (ΔS^{θ}) from the variations of K_L and temperature. Because K_L is equilibrium constant, its dependence on temperature can be used to predict thermodynamic parameters including changes in adsorption-associated ΔG^{θ}, ΔH^{θ} and ΔS^{θ}, which were determined as follows:

$$\Delta G^{\theta} = -RT \times \ln K_L \tag{9}$$

$$\Delta H^{\theta} = \Delta G^{\theta} + T \times \Delta S^{\theta} \tag{10}$$

where R is the universal gas constant (8.314 J mol^{-1} K^{-1}) and T is the adsorption temperature.

3. RESULT AND DISCUSSION

3.2 Characterization of biochar samples

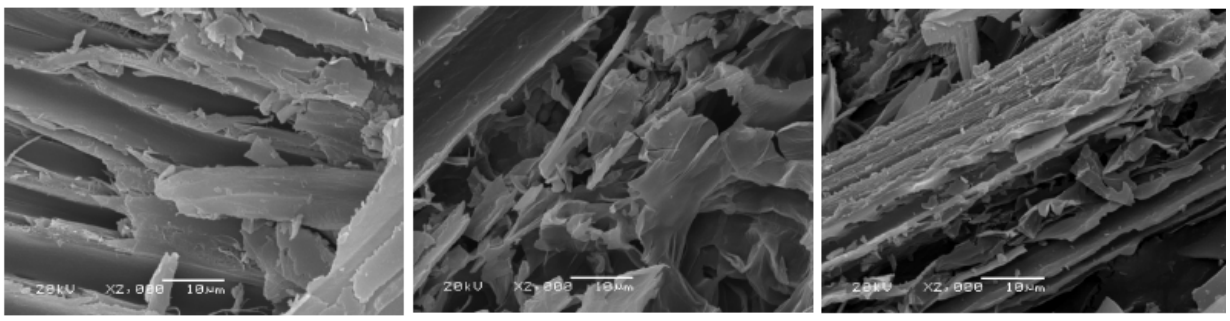

Figure 1 SEM images of biochar samples at varying pyrolytic temperatures

Three biochar samples were obtained from wheat residue at varying pyrolytic temperature. The surface SEM shows that temperature is a key factor affecting the surface feature of biochar (Figure 1). When the biochar samples were carbonized at low temperature, the pore channels of the straw were regularly and evenly distributed. The surface feature changed significantly with the temperature rise. At 400 °C, a part of the pore channels was carbonized into pieces, which was more obvious at 600 °C (Figure 1). When the carbonizing temperature exceeded 400 °C, the micro-pore walls were burnt

as they were molten, which exacerbated the surface roughness of biochar (Figure 1). The results may be explained that the porous edges of the straw were melted during the carbonization. When the straw was heated, abundant energy was released to open the inner pores, which disordered the distribution of straw pore and improved the surface roughness of biochar.

The properties of biochar surface affected by pyrolytic temperature were further illustrated by FTIR data in Figure 2. The spectra of biochar are primarily characterized at wavenumber of 3428, 2922, 1702/1605, 1429, 1225 and 1057 cm^{-1}, which are assigned respectively to the hydroxyl (–OH) stretching, the methylene ($–CH_2–$) stretching, the aromatic carboxyl/carbonyl (–C=O) stretching, the –COOH and –CHO stretching, the aromatic CO– and phenolic –OH stretching, and the C–O–C stretching. Most of the bands appeared with high intensity for BC-200, but the band intensity was gradually weakened for BC-400 and BC-600 with increasing pyrolytic temperature from 200 to 600 ℃ and some bands (e.g. methylene $–CH_2–$, –COOH, –CHO, phenolic –OH, and C–O–C) disappeared at higher temperature. The amount of acidic groups decreased with increasing temperature, and the acidic groups also were nearly absent at higher temperature (Figure 2). For instance, the band at 1057 cm^{-1} disappeared when the pyrolytic temperature was raised from 200 to 400 or 600 °C, indicating that the cellulose was decomposed and C–O–C was broken. The band at 1605 cm^{-1} for the stretching of aromatic C=O ring may reflect both acidic and basic groups, whose intensities were improved at 400 and 600 °C, which probably resulted from an increase in basicity with pyrolytic temperature (Chun et al. 2004).

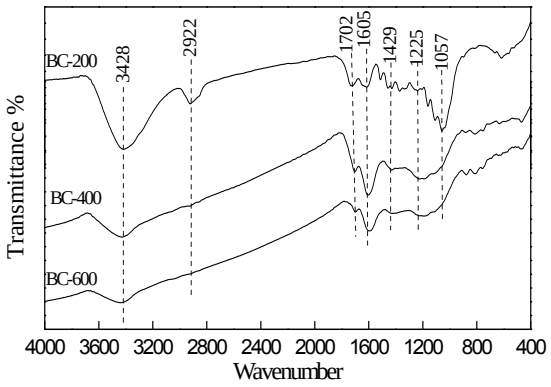

Figure 2 FTIR spectra of biochar samples

3.2 Adsorption kinetic

To investigate the potential rate-controlling steps involved in the adsorption of naphthalene onto biochar, pseudo-first-order kinetic, pseudo-second-order kinetic and intraparticle diffusion models were used to fit the experimental data. Table 1 listed the calculated results from three models based on Eq. (1), Eq. (2), and Eq. (3). The correlation coefficients for the second-order kinetic model were equal to 1 for almost all the cases. The calculated values agreed well with the experimental data, indicating that the adsorption system obeyed the pseudo-second-order kinetic model.

Table 1 Eigenvalue for the kinetic sorption equation of naphthalene by biochar

	Pseudo-first-order equation			Pseudo-second-order equation			Intraparticle equation		
	k_1	q_1	r_1^2	k_2	q_2	r_2^2	k_p	c	r_p^2
BC-200	0.469	39.4	0.872	0. 0208	43.3	0.999	2.75	24.5	0.794
BC-400	0.131	45.2	0.987	0.0909	45.7	1.000	0.902	39.7	0.740
BC-600	0.0234	46.7	0.940	0.223	47.4	1.000	0.298	45.3	0.819

Figure 3 shows the effect of adsorption time on the adsorption capacities of naphthalene by biochar. It was clear that the adsorption capacities of naphthalene increased rapidly with the increase of adsorption time from 0 to 2 h and more than 90% of the equilibrium adsorption capacities of naphthalene occurred within 2 h. It could be seen from Figure 3 that the adsorption capacities of naphthalene gradually increased with the increase of the adsorption time from 0.5 to 2 h until equilibrium. Because the biochar had relatively high-equilibrium adsorption capacity, the adsorption rate became very fast, and thus the required equilibrium time was short (Figure 3). The short equilibrium time coupled with high adsorption capacity indicated a high-degree affinity of the biochar samples with the naphthalene. Besides, the adsorption capacity was improved with the rise of pyrolytic temperature for biochar. Our result may be explained that the biochar produced at a high temperature was more effective for adsorption of naphthalene because of its high surface area and micropore development, which induced a very fast adsorption rate of BC-600 than BC-200 and BC-400.

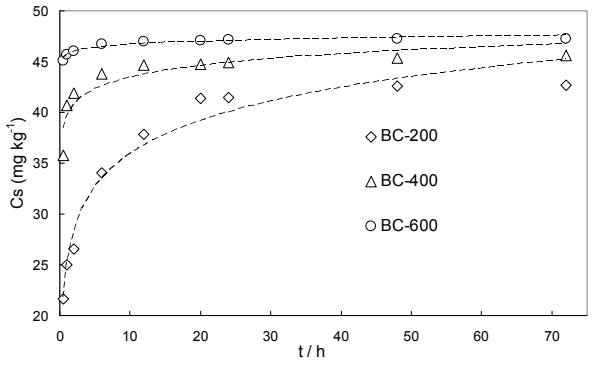

Figure 3 Kinetic sorption of naphthalene by biochar at varying temperatures

Figure 4 shows effect of the adsorption of different initial naphthalene concentrations onto the biochar at 25℃. As the initial naphthalene concentration increases from 19.2 to 32 mg L^{-1} the equilibrium adsorption capacity of naphthalene increases from 42.6 to 69.6 mg g^{-1}. The equilibrium adsorption capacities of naphthalene occurred within 2 h. It was clear that the similar curve of adsorption kinetics of naphthalene onto the biochar were found at different initial naphthalene concentrations. This may be attributed to an increase in the driving force of the concentration gradient with the increase in the initial naphthalene concentration in order to overcome all mass transfer resistance of naphthalene between the aqueous and solid

phases. Therefore, a higher initial concentration of naphthalene may increase the adsorption capacity. Besides, a higher initial concentration of naphthalene may not change the kinetic sorption process.

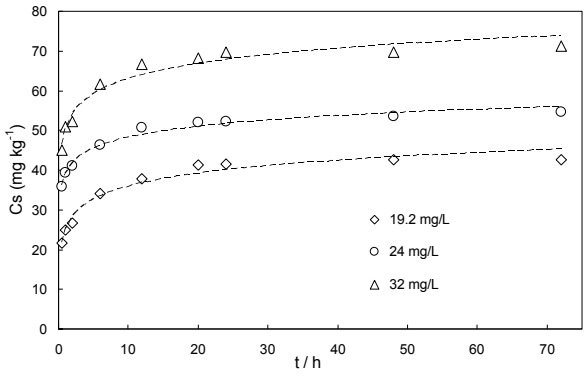

Figure 4 Kinetic sorption of naphthalene by biochar at varying initial concentration

However, the pseudo-first-order and pseudo-second-order kinetic models could not identify the diffusion mechanism, so the kinetic results were also analyzed by using the intraparticle diffusion model. According to this model, the plot of uptake, q_t, versus the square root of time ($t^{1/2}$) should be linear if intraparticle diffusion is involved in the adsorption process and if these lines pass through the origin then intraparticle diffusion is the rate-controlling step (Chen et al. 2003). Furthermore, if the plots do not pass through the origin, this is indicative of some degree of boundary layer control and the intraparticle diffusion is not the only rate-limiting step, and all of which may be operating simultaneously (Özcan et al. 2005). From the Figure 5, the plot of uptake, q_t, versus the square root of time ($t^{1/2}$) were linear, and the correlation coefficients obtained are greater than 0.952. This indicates that intraparticle diffusion is involved in the adsorption process. The plots do not pass through the origin, which mean the boundary layer control is involved in the adsorption process.

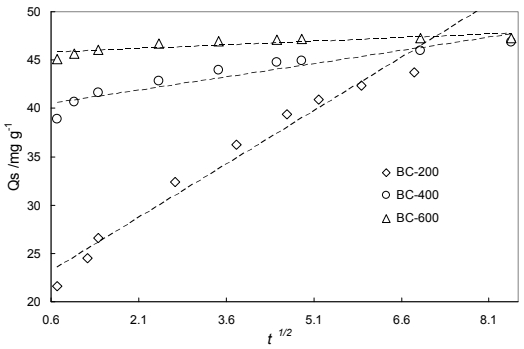

Figure 5 Intraparticle diffusion plots for adsorption of naphthalene by biochar

3.3 Adsorption thermodynamic

All the constants are determined based on Eq. (4), Eq. (5), and Eq. (6), and their value as well as their correlation coefficients is presented in Table 2. As seen from Table 2, the correlation coefficients (R^2) of model indicated that the Freundlich isotherm model fitted the equilibrium data for naphthalene adsorption significantly better than the Langmuir isotherm model. The fact might be due to heterogeneous surfaces of the adsorbent, because the Freundlich equation assumes that the surface is heterogeneous, which indicates the multilayer adsorption of naphthalene onto biochar.

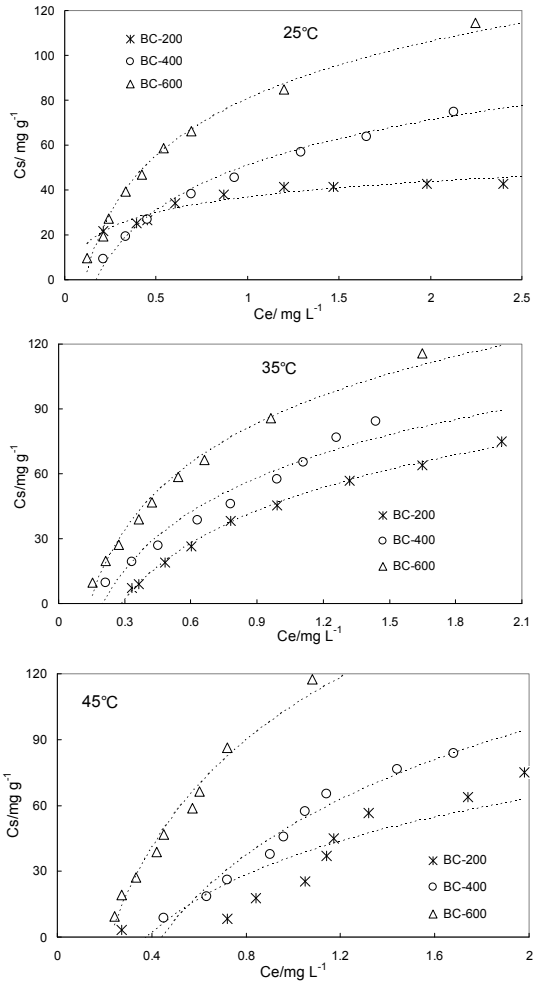

Figure 6 Adsorption isotherms of naphthalene by biochar samples at varying temperatures

From Figure 6 and Table 2, q_m increased as the temperature was increased from 303 to 353 K, which showed that the processes are endothermic. Besides, q_m increases with increase of the pyrolytic temperature of biochar. The biochar produced at 500-700°C was well carbonized with a relatively high surface area, but the biochar formed at 300-400°C was only partially carbonized (Chun et al. 2004). Our result may

be explained that the wheat straw was not completely carbonized when the biochar was prepared at low temperature (200 and 400°C), but the biochar produced at a high temperature was more effective for adsorption of naphthalene because of its high surface area and micropore development.

The mean free energy of adsorption, E (kJ mol^{-1}), was connected with D-R adsorption isotherm and calculated from Eq. (7). The E increased from 1.30 to 3.41 kJ mol^{-1} when the temperature increased from 25 to 45℃, which indicated a physical sorption. The separation factor, R_L, is used to reveal the essential characteristics of Langmuir isotherm and calculated from Eq. (8). R_L indicates the isotherm shape and whether the adsorption is favorable or not: unfavorable (R_L > 1), linear (R_L = 1), favorable (0 < R_L < 1), or irreversible (R_L = 0). R_L ranged from 0.0235 to 0.292 at varying temperature, indicating that the adsorption of naphthalene by biochar is favorable (Fasfous et al. 2010). Besides, the R_L at all temperatures ranged from 0.0235 to 0.292, which suggested the spontaneous adsorption.

Table 2 Eigenvalue of isothermal adsorption equation of naphthalene by biochar

		D-R equation				Freundlich equation			Langmuir equation			
		$\ln q_m$	B ($\times 10^{-8}$)	r^2	E	K_F	n	r^2	K_L	Q_m	r^2	R_L
25℃	BC-200	3.77	4.31	0.942	3.41	0.192	3.23	0.933	0.299	49.0	0.924	0.122
	BC-400	4.32	11.5	0.981	2.09	0.216	1.24	0.959	0.472	149	0.940	0.0567
	BC-600	4.65	8.25	0.967	2.46	0.278	1.22	0.917	0.566	172	0.908	0.0235
35℃	BC-200	4.48	19.6	0.997	2.60	0.202	0.798	0.930	0.301	151	0.981	0.292
	BC-400	4.47	11.8	0.973	2.06	0.249	0.907	0.991	0.519	434	0.975	0.193
	BC-600	4.78	9.39	0.995	2.31	0.293	0.997	0.934	0.636	714	0.919	0.133
45℃	BC-200	4.12	19.6	0.977	1.60	0.150	0.581	0.942	0.440	361	0.935	0.0865
	BC-400	4.89	29.5	0.987	1.30	0.215	0.564	0.955	0.551	472	0.965	0.0592
	BC-600	5.21	14.8	0.979	1.84	0.329	0.634	0.939	0.765	813	0.903	0.0304

3.4 Analysis of thermodynamic parameters

The obtained thermodynamic parameters for naphthalene adsorption onto biochar were listed in Table 3. The adsorption on solids is classified into physical adsorption and chemical adsorption. Physical adsorption is nonspecific, and the variation of energy for physical adsorption is usually substantially smaller than that of chemical adsorption. Chemical adsorption is similar to ordinary chemical reactions in which it is highly specific. Typically, ΔH^{θ} for physical adsorption ranges from 24 to 240 kJ/mol, which is relatively smaller compared to that of chemical adsorption ranging from 240 to 2800 kJ/mol [12]. As shown in Table 3, the ΔH^{θ} values suggested that the adsorption process might be considered to be a physical adsorption.

The negative values of ΔG^{θ} indicated that the adsorption of naphthalene onto biochar was spontaneous. Therefore, the positive values of ΔS^{θ} suggested the affinity of the naphthalene for the biochar, and the increase of randomness at the solid/liquid interface during adsorption process might be due to the release of water molecules produced by molecule exchange between naphthalene and the functional groups attached on the biochar surface.

Table 3 Thermodynamic parameters calculated from Langmuir isotherm constant (K_L) for the adsorption of Naphthalene by biochar

	T/K	ΔG^{θ} /kJ·mol^{-1}	ΔH^{θ}/kJ·mol^{-1}	ΔS^{θ}/J·(mol·K)$^{-1}$
BC-200	298.15	-15.0	-7.56	30
	308.15	-15.3		
	318.15	-15.5		
BC-400	298.15	-13.8	-4.86	25
	308.15	-14.1		
	318.15	-14.4		
BC-600	298.15	-13.4	-4.61	10
	308.15	-13.5		
	318.15	-13.6		

4. CONCLUSIONS

The biochar produced from wheat residue have a strong effect on the adsorption of naphthalene. The surface feature and the chemical structure of biochar were modified at varying pyrolytic temperature. The adsorption kinetics of naphthalene best conformed to the pseudo-second-order kinetics equation, and the boundary layer control and intraparticle diffusion are involved in the adsorption simultaneously. The Freundlich isotherm model fitted the equilibrium data for naphthalene adsorption significantly better than the Langmuir isotherm model, indicating a multilayer adsorption of naphthalene onto biochar. The adsorption capacity was improved with the increase of system temperature, indicating that the adsorption was an exothermic process. ΔG^{θ} was negative at all temperatures, confirming that the adsorption of naphthalene onto biochar was spontaneous and thermodynamically favorable. The thermodynamic parameters analyses show that the adsorption is mainly physical sorption.

REFERENCES

Ahmad, M., Lee, S.S., Dou, X., Mohan, D., Sung, J.K., Yang, J.E. and Ok, Y.S. (2012), "Effects of pyrolysis temperature on soybean stover- and peanut shell-derived biochar properties and TCE adsorption in water", *Bioresour. Technol.,* Vol.**118**, 536-544.

Ahmad, M., Lee, S.S., Rajapaksha, A.U., Vithanage, M., Zhang, M., Cho, J.S., Lee, S. and Ok, Y.S. (2013), "Trichloroethylene adsorption by pine needle biochars produced at various pyrolysis temperatures", *Bioresour. Technol.,* Vol.**143**, 615-622.

Ahmad, M., Rajapaksha, A.U., Lim, J.E., Zhang, M., Bolan, N., Mohan, D. and Ok, Y.S. (2014), "Biochar as a sorbent for contaminant management in soil and water: A review", *Chemosphere*, Vol.**99**, 19-33.

Cao, X., Ma, L., Liang, Y., Gao, B. and Harris, W. (2011), "Simultaneous immobilization of lead and atrazine in contaminated soils using dairy-manure biochar", *Environ. Sci. Technol.,* Vol.**45**, 4884-4889.

Chen, J.P., Wu, S. and Chong, K.H. (2003), "Surface modification of a granular activated carbon by citric acid for enhancement of copper adsorption", *Carbon*, Vol.**41**, 1979-1986.

Chun, Y., Sheng, G., Chiou, C.T. and Xing, B. (2004), "Compositions and sorptive properties of crop residue-derived chars", *Environ. Sci. Technol.,* Vol.38, 4649-4655.

Dubinin, M.M., Zaverina, E.D. and Radushkevich, L.V. (1947), "Sorption and structure of active carbons. I. Adsorption of organic vapors", *Zh. Fiz. Khim.,* Vol.**21**, 1351-1362.

Fasfous, I.I., Radwan, E.S. and Dawoud, J.N. (2010), "Kinetics, equilibrium and thermodynamics of the sorption of tetrabromobisphenol A on multiwalled carbon nanotubes", *Appl. Surf. Sci.,* Vol.**256**, 7246-7252.

Freundlich, H. (1906), "Uber die adsorption in losungen (Adsorption in solution)", *Z. Phys. Chem.,* Vol.**57**, 384-470.

Helfferich, F. (1979), "Ion exchange", NY, USA: McGraw Hill.

Ho, Y.S. and McKay, G. (1998a), "Sorption of dye from aqueous solution by peat", *Chem. Eng. J.,* Vol.**70**,115-124.

Ho, Y.S. and McKay, G. (1998b), "The kinetics of sorption of basic dyes from aqueous solution by sphagnum moss peat", *Can. J. Chem. Eng.,* Vol.**76**, 822-827

Ho, Y.S. and McKay, G. (1998c), "Kinetic models for the sorption of dye from aqueous solution by wood", *J. Environ. Sci. Health. Part B: Process Saf. Environ. Prot.,* Vol.**76**(B2),183-191.

Kiran, I., Akar, T., Ozcan, A.S., Ozcan, A. and Tunali, S. (2006), "Biosorption kinetics and isotherm studies of Acid Red 57 by dried Cephalosporium aphidicola cells from aqueous solutions", *Biochem. Eng. J.,* Vol.**31**, 197-203.

Langmuir, I. (1918), "The adsorption of gases on plane surfaces of glass, mica and platinum", *J. Am. Chem. Soc.,* Vol.**40**, 1361-1403.

Mohan, D., Sarswat, A., Ok, Y.S. and Jr. Pittman, C.U. (2014), "Organic and inorganic contaminants removal from water with biochar, a renewable, low cost and sustainable adsorbent-a critical review", *Bioresour. Technol.,* Vol.**160**, 191-202.

Lehmann, J. and Joseph, S. (2009), "Biochar for Environmental Management: Science and Technology", London: Earthscan

McKay, G., Blair, H.S. and Gardener, J.R. (1982), "Adsorption of dyes on chitin I, Equilibrium studies", *J. Appl. Polym. Sci.,* Vol.**27**, 3043-5307.

Özcan, A., Özcan, A.S., Tunali, S., Akar, T. and Kiran, I. (2005), "Determination of the equilibrium, kinetic and thermodynamic parameters of adsorption of copper(II) ions onto seeds of Capsicum annuum", *J. Hazard. Mater.,* Vol.**B124**, 200-208.

Sun, K., Jin, J., Keiluweit, M., Kleber, M., Wang, Z., Pan, Z. and Xing, B. (2012), "Polar and aliphatic domains regulate sorption of phthalic acid esters (PAEs) to biochars", *Bioresour. Technol.,* Vol.**118**, 120-127.

Uchimiya, M., Wartelle, L.H., Lima, I.M. and Klasson, K.T. (2010), "Sorption of deisopropylatrazine on broiler litter biochars", *J. Agric. Food Chem.,* Vol.**58**, 12350-12356.

Uchimiya, M., Chang, S. and Klasson, K.T. (2011), "Screening biochars for heavy metal retention in soil: role of oxygen functional groups", *J. Hazard. Mater.,* Vol.**190**, 432-441.

Weber Jr., W.J. and Morriss, J.C. (1963), "Kinetics of adsorption on carbon from solution", *J. Sanitary Eng. Div. Am. Soc. Civ. Eng.,* Vol.**89**, 31-60.

Yang, Y. and Sheng, G. (2003), "Enhanced pesticide sorption by soils containing particulate matter from crop residue burns", *Environ. Sci. Technol.,* Vol.**37**, 3635-3639.

Zhang, P., Sun, H., Yu, L. and Sun, T. (2013), "Adsorption and catalytic hydrolysis of carbaryl and atrazine on pig manure-derived biochars: **Impact** of structural properties of biochars", *J. Hazard. Mater.,* Vol.**244–245**, 217-224.

Zhao, X., Ouyang, W., Hao, F., Lin, C., Wang, F., Han, S. and Geng, X. (2013), "Properties comparison of biochars from corn straw with different pretreatment and sorption behaviour of atrazine", *Bioresour. Technol.,* Vol.**147**, 338-344.